

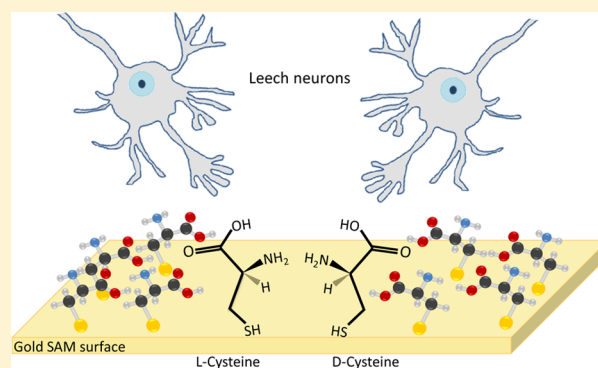
Neuronal Growth on L- and D-Cysteine Self-Assembled Monolayers Reveals Neuronal Chiral Sensitivity

Koby Baranes,^{†,||} Hagay Moshe,^{‡,||} Noa Alon,^{†,||} Shmulik Schwartz,^{†,§,||} and Orit Shefi^{*,†,||}[†]Faculty of Engineering, [‡]Department of Chemistry, [§]Gonda Multidisciplinary Brain Research Center, and ^{||}Bar Ilan Institute of Nanotechnologies and Advanced Materials, Bar Ilan University, 5290002 Ramat Gan, Israel

Supporting Information

ABSTRACT: Studying the interaction between neuronal cells and chiral molecules is fundamental for the design of novel biomaterials and drugs. Chirality influences all biological processes that involve intermolecular interaction. One common method used to study cellular interactions with different enantiomeric targets is the use of chiral surfaces. Based on previous studies that demonstrated the importance of cysteine in the nervous system, we studied the effect of L- and D-cysteine on single neuronal growth. L-Cysteine, which normally functions as a neuromodulator or a neuroprotective antioxidant, causes damage at elevated levels, which may occur post trauma. In this study, we grew adult neurons in culture enriched with L- and D-cysteine as free compounds or as self-assembled monolayers of chiral surfaces and examined the effect on the neuronal morphology and adhesion. Notably, we have found that exposure to the L-cysteine enantiomer inhibited, and even prevented, neuronal attachment more severely than exposure to the D-cysteine enantiomer. Atop the L-cysteine surfaces, neuronal growth was reduced and degenerated. Since the cysteine molecules were attached to the surface via the thiol groups, the neuronal membrane was exposed to the molecular chiral site. Thus, our results have demonstrated high neuronal chiral sensitivity, revealing chiral surfaces as indirect regulators of neuronal cells and providing a reference for studying chiral drugs.

KEYWORDS: Neuronal growth, chirality, cysteine, neurotoxicity, SAMs, leech



Chirality is a major aspect in the design, discovery, and development of novel biomaterials and drugs. The discovery of the importance of stereochemistry in biochemical environments dates back to 1860, when Pasteur reported on the different destruction rates of *dextro* and *levo* ammonium tartrate by the mold *Penicillium glaucum*.¹ It was found that amino acids are all L-enantiomers, whereas most of the sugars have the D-configuration. Thus, chirality, which represents an intrinsic property of the “building blocks of life”, influences all biological processes that involve intermolecular interactions, demonstrating sensitivity to stereochemistry.^{2–5}

A common method to study interactions of cells with different enantiomeric targets is the use of chiral surfaces.^{6,7} Surfaces can be considered chiral if they are based on chiral crystals or on templates with chiral molecules.⁸ Hanein et al. have examined the interaction of epithelial cells with chiral crystals, and showed that cells attach in a different manner to the two crystal enantiomer surfaces, thus demonstrating sensitivity to surface chirality on the angstrom scale.⁹ They reported differential adhesion of epithelial cells to enantiomorphous crystal surfaces of the [011] faces of the (R,R)- and (S,S)-calcium tartrate tetrahydrate. Moreover, they found that cell attachment to the chiral crystal surface is not followed by normal cell spreading and development of focal adhesions, but results in massive cell death.¹⁰ These stereospecific behaviors

were reported for additional types of cells, including immune cells, affecting cell–substrate interaction and cell adhesion.^{11–15} Interestingly, when administering the two enantiomers in solution to the cell medium, no effect on their adhesion and growth was detected, when compared to the regular medium.⁹

Previous studies have demonstrated stereoselectivity of neuronal tissue, with high functional sensitivity to chirality.¹⁶ In this work, we studied the influence of molecular chiral configuration and chiral surface interaction on single neuronal cells. We examined chiral surfaces based on cysteine, since it has been known to play an important role in neuronal tissues and in the brain. L-Cysteine (L-Cys) is a precursor for the synthesis of glutamate-cysteine-glycyltripeptide (glutathione, GSH), a neuroprotective antioxidant.^{17–19} Low levels of L-Cys are required for normal neuronal function.²⁰ Recent studies have also suggested a role of L-Cys as a neuromodulator in neuronal activity,^{21–24} affecting N-methyl-D-aspartate (NMDA) gated currents.^{25–27} On the other hand, elevated levels of L-Cys lead to damage and a neurotoxic effect which may injure neurons^{28–33} (reviewed by Janáky et al.³⁴). Evidence exists that high levels of L-Cys may develop following neuronal trauma such as brain ischemia.³⁵

Received: December 13, 2013

Published: February 24, 2014



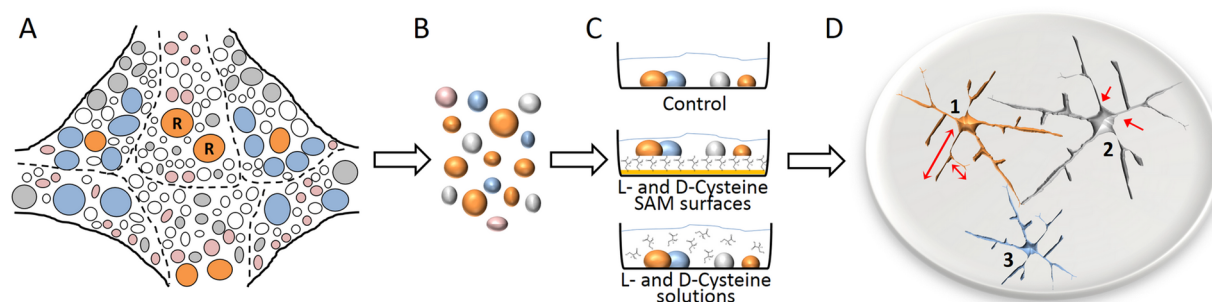


Figure 1. Schematic drawing of the experimental setup. (A) Ganglia are dissected from the leech CNS. Retzius (R) cells are marked for orientation. (B) Ganglia were dissociated, and the neuronal cells were removed from the ganglia. (C) Neurons were plated atop the various surfaces. (D) Morphometric parameters were measured and analyzed including the number of cells, number of cells with neurites, and the total branching tree length.

The importance of *L*-cysteine in brain function, and its wide range of effects, from a neuroprotective to a neurotoxic reagent, raises the question as to how neurons interact with cysteine, and whether there is a difference between the two cysteine enantiomers. Moreover, how cysteine and cysteine-based chiral surfaces may affect neuronal growth and regeneration is significant for the development of therapeutic applications.

We have grown adult neurons in culture, interacting with *L*-Cys and *D*-Cys as free compounds or as chiral surfaces, at different concentrations. We used primary neurons of a simple model, the medicinal leech that allows a detailed morphological analysis at the single cell level to study the effect of the two enantiomers. We used well-defined self-assembled monolayers (SAMs) of *L*- and *D*-Cys on gold surfaces as the growth substrates (as described in the Methods and in previous articles^{6,7}). We studied a graded influence of cysteine, examining the toxic effect of high levels of *L*-Cys as detected post-trauma. Comparing the *L*-Cys effect with the influence of *D*-Cys on the neuronal growth enabled us to examine whether the effect can be masked. Thus, our study may contribute to the understanding of cysteine–neuron interactions and neuronal chiral sensitivity.

RESULTS AND DISCUSSION

The Role of Cysteine in the Nervous System. In the nervous system, *L*-Cys is related to the modulation of neuronal activity. Keller and coauthors have shown that *L*-Cys is released from rat brain slices upon depolarization in a Ca^{2+} -dependent manner.²¹ In nociceptive neurons *in vitro*, *L*-Cys augments T-type currents, which are voltage-gated calcium channels.^{36,37} *L*-Cys lowers the threshold for excitability, thus inducing T-type Ca^{2+} channel-dependent burst firing.²² Cysteine residues can selectively activate NMDA receptors at low concentrations^{26,27} and have led to inhibition of glutamate reuptake and to neuronal excitation.³⁸ These results suggest that cysteine is released from neuronal compartments and may be involved in neurotransmission, acting as a neuromodulator. Under normal physiological conditions, *L*-Cys, which is the natural configuration of cysteine, has a protective role against neurotoxicity.^{39–41} However, a review by Janáky et al.³⁴ presents a possible neurotoxicity effect of *L*-Cys which may injure neurons. Several studies linked neuronal trauma with elevated levels of *L*-Cys in the central nervous system (CNS). During brain ischemia in gerbils, the levels of cysteine rise above normal levels while levels of GSH fall.³⁵ Interestingly, a cysteine-rich intestinal protein, HmCRIP, which is an important factor in the

regulation of the inflammatory immune response, is upregulated after axotomy in leech neurons.⁴² Thus, the study of the role of cysteine in neuronal growth and the effect of cysteine on neuronal outgrowth morphology is important and has not yet been reported.

We studied the neurite outgrowth of adult neurons from leech dissociated ganglia treated with cysteine or attached to cysteine SAM surface. Previous studies have demonstrated the sensitivity of the nervous system to chiral configuration.^{43,44} Chiral enantiomers were developed as safer alternatives to medical drugs.⁴⁵ We tested the interaction of both *L*-Cys and *D*-Cys with the neurons. We grew primary leech neurons on chiral SAM surfaces with *L*-Cys and *D*-Cys and in regular culture medium enriched with *L*-Cys and *D*-Cys (low and high concentrations of 2 and 10 mM respectively, see experimental sections). For each condition we measured the neuronal morphology and adhesion rate and compared it to the cultures with no supplemented cysteine, as described in Baranes et al.⁴⁶ The adhesion and neuronal morphology were traced for several days and up to a week (Figure 1). We consider morphometric analysis as a useful tool to quantify the effect of the different treatments on neurons and as a method to evaluate the influence on neuronal state and outgrowth. In addition, we performed electrophysiological recordings of single neurons in culture, before and after supplementing cysteine to the medium (*L*-Cys and *D*-Cys); see the Supporting Information.

Neurons Growing in Culture Media Enriched with *L*- and *D*-Cys Solutions. In control cultures, one day after plating, almost 40% of the plated neurons were attached to the substrates (no cysteine). For 20% of the attached neurons, neurites have initiated from the soma (Figure 2A,B, left set of bars, light blue). Figure 2A demonstrates the effect on neuronal adhesion following the addition of *L*-Cys and *D*-Cys to the medium. One day after plating, in low-*D*-Cys solution, a slightly lower percentage of neurons was attached to the substrates than in the control plates (no significant difference). For cultures enriched with *L*-Cys, less neurons were attached to the substrates than for both control and cultures enriched with *D*-Cys ($25 \pm 2\%$ and $30 \pm 4\%$, respectively). For the higher concentrations of *L*-Cys and *D*-Cys, only 5% and 8% of the plated neurons were attached to the substrates, respectively. As for the percentage of neurons with neurites, after one day in culture, both low-*L*-Cys and low-*D*-Cys had similar percentages as the control ($22 \pm 4\%$, $24 \pm 3\%$, and $22 \pm 1\%$, respectively (Figure 2B, left bars)). No neurites grew in cultures supplemented with high concentrations of *L*-Cys and *D*-Cys.

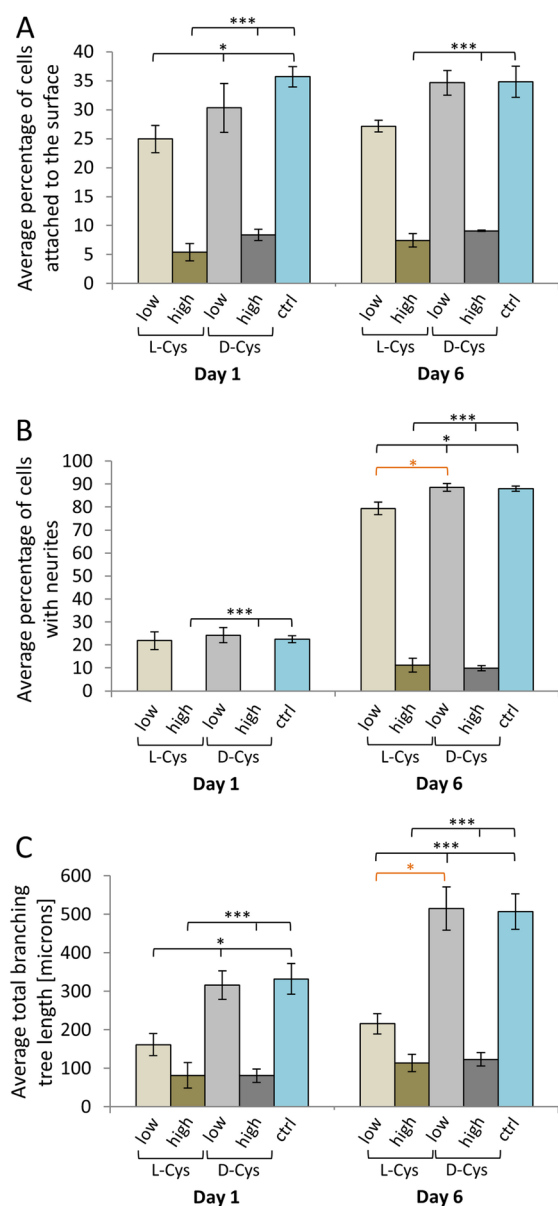


Figure 2. Statistics for neurons treated with medium supplemented with L- and D-Cys solutions. (A) Average percentage of cells attached to the substrates for the low and high concentrations of L-Cys and D-Cys and for the control, 1 day and 6 days after plating. (B) Average percentage of cells with neurites, for the low and high concentrations of L-Cys and D-Cys, and for the control, 1 day and 6 days after plating. Significant differences are seen between L-Cys and D-Cys for the lower concentration on day 6. (C) Average total branching tree length for the low and high concentrations of L-Cys and D-Cys, and for the control, 1 day and 6 days after plating. Scheffe test, labeled in orange, compares two conditions $*p < 0.05$; GLM test, labeled in black, was used for multiple groups, $*p < 0.05$, $**p < 0.005$, $***p < 0.001$.

Six days after plating, the adhesion rate was still 35% for the control cultures. Almost 90% of the attached neurons initiated neurites (Figure 2A, B, right set of bars, light blue). For cultures supplemented with low concentration of D-Cys, the adhesion rate and percentage of neurons with neurites were similar (35% attached neurons, 89% of which are with neurites). For cultures supplemented with low-L-Cys, the adhesion rate was lower (27%). For the high concentrations of D-Cys and L-Cys, the adhesion rates were even lower than 10% (7% for high-L-Cys

and 9% for high-D-Cys). Again, addition of L-Cys to the medium suppressed growth and led to significantly less neurites than for neurons treated with D-Cys

Figure 2C demonstrates the average total branching tree length for the control and treated neurons. We found that after one day in culture, the average total branching tree length of neurons growing in medium conditioned with low-L-Cys is almost half of that of neurons supplemented with low-D-Cys ($161 \pm 28 \mu\text{m}$ and $315 \pm 37 \mu\text{m}$, respectively). It can be seen that neurons in the low-D-Cys cultures developed similar branching tree length to neurons in the control cultures. For both high-L-Cys and high-D-Cys cultures, the average total branching tree lengths were significantly lower (Figure 2C).

Similar trends were measured after 6 days in culture. It can be seen that neurons in the low-D-Cys cultures developed similar branching tree length as the control, and significantly longer than the low-L-Cys ($p < 0.05$, Scheffe test), as well as the high concentrations (Figure 2C).

The results presented in Figure 2 demonstrate an inhibiting effect of L-Cys on neuronal growth that seems to reduce and even prevent neuronal attachment and growth. The effect is chiral sensitive and the exposure of neurons to D-Cys has led to less damage; the morphometric parameters we measured for neurons treated with low-D-Cys were similar to those of the control plates. We also demonstrated a concentration-dependent effect. The attachment and growth of neurons in the presence of 10 mM L-Cys and D-Cys that are considered high toxic concentrations were reduced in comparison to the 2 mM concentration which is close to the cysteine levels post neuronal trauma.³⁵

In previous studies, the effect of the two enantiomers of cysteine on cellular attachment has been examined for non-neuronal systems. Gillin and Diamond examined the effect of the addition of L-Cys and D-Cys to the growth medium on the attachment of the parasite *Entamoeba histolytica* to glass. No differences between the cultures enriched with L-Cys and D-Cys were found.⁴⁷ Gazit et al. demonstrated possible damage to neuronal tissue of the natural configuration of cysteine, L-Cys. They showed that L-Cys injection into mice can cause pronounced hypoglycemia and central neural damage.²⁸

Neurons Growing atop L-Cys and D-Cys SAM Surfaces.

Next, we studied the influence of L-Cys and D-Cys SAM surfaces on neuronal growth. High resolution scanning electron microscopy (HR-SEM) micrographs of neurons atop the SAM surfaces demonstrate less adhesion and dendritic growth for neurons growing atop the L-Cys surfaces compared to neurons growing atop the D-Cys surfaces (Figure 3, upper panels). Fewer neurites grew out of the cell soma, and the branching tree is less developed. Zooming into the branching tree region shows short degenerated neurites atop the L-Cys surfaces, and long and developed neurites atop the D-Cys surfaces (Figure 3, lower panels).

A quantitative analysis of the adhesion rate of the neurons after one day in culture atop the L-Cys and D-Cys SAM surfaces demonstrates no significant effect on the neuronal growth. However, by day 6, neurons atop the D-Cys surfaces attached to the surface at a similar rate as those of the control cultures, and significantly higher than those atop the L-Cys surfaces ($35 \pm 3\%$ vs $21 \pm 3\%$, low concentration coatings, day 6, $p < 0.05$, Scheffe test) (Figure 4A). Figure 4B shows that, after one day, there was an outgrowth of almost no neurites for neurons atop the SAM surfaces, an amount significantly less than the control ($2 \pm 1\%$, $2 \pm 1\%$ and $23 \pm 1\%$, respectively, $p < 0.001$, GLM test).

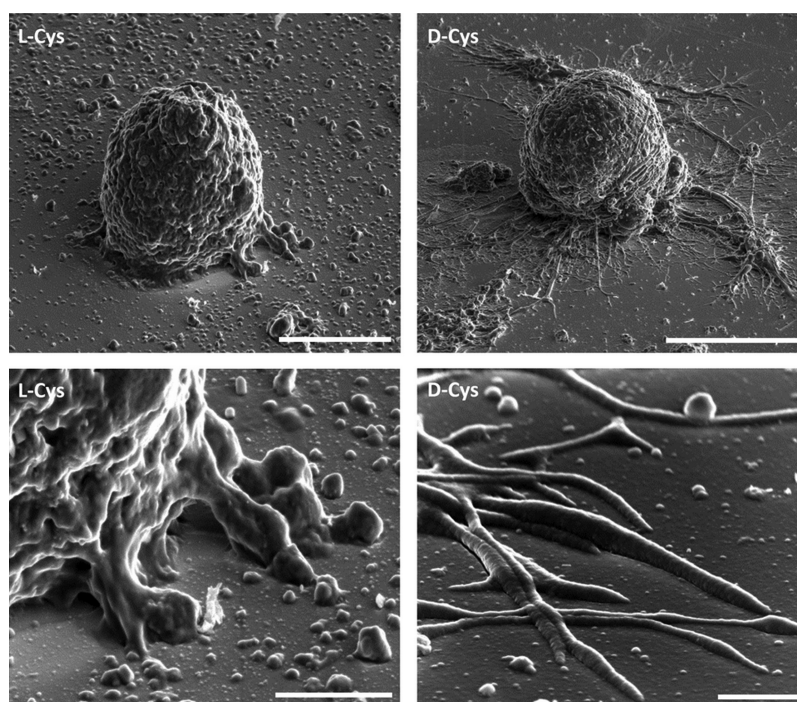


Figure 3. Neurons growing atop L-Cys and D-Cys SAM surfaces. HR-SEM micrographs of 6 day old neurons growing atop L-Cys (left panels) and D-Cys (right panels). Upper panels present the whole neurons. Scale bars are 10 μm (left) and 20 μm (right). Lower panels show zoomed-in images of the neurite region in the upper panels. Scale bars are 3 μm (left) and 1 μm (right).

Six days after plating, $27 \pm 5\%$ of the neurons atop the low-D-Cys surfaces developed neurites, while only $12 \pm 6\%$ developed neurites atop the low-L-Cys ($88 \pm 1\%$ atop the control, $p < 0.001$, GLM test).

Growth atop the two chiral SAM surfaces affected the outgrowth and the total branching tree length differently. It can be seen that neurons atop the D-Cys surfaces developed longer branching trees than neurons atop the L-Cys surfaces ($504 \pm 48 \mu\text{m}$ vs $318 \pm 46 \mu\text{m}$, 6 days, low-concentration coating) (Figure 4C). Interestingly, the branching tree length on the D-Cys surfaces resembled the branching tree length of the control neurons ($506 \pm 46 \mu\text{m}$).

For SAM surfaces with high concentrations of L- and D-Cys, the statistics of the morphological parameters were similar to those of the high-L-Cys and high-D-Cys solutions.

Our results for interaction of neurons with L-Cys and D-Cys SAMs demonstrate a clear effect on the attachment and adhesion of neurons to surfaces. The L-Cys coating reduces the ability of neurons to attach to the surface and to develop optimized branching trees. These results are opposed to previous studies of the interaction of non-neuronal cells with Cys-treated surfaces. Fibroblast cells grown atop gold surfaces coated with cysteine of both chiral configurations (L- and D-) demonstrated better adhesion to the L-Cys assembled surfaces than to the D-Cys surfaces.⁴⁸ Interaction of immune cells with chiral surfaces of L- and D-NIBC (*N*-isobutyryl-L(D)-cysteine) molecules also led to different adhesion and morphology of the cells, presenting better attachment to the L-Cys coated surfaces.¹³ A recent study using mesenchymal stem cells has shown an effect similar to that of fibroblast cells. The density of the cells was higher on the L-Cys-coated surface than on the D-Cys enantiomer, and cells adhesion was enhanced.⁴⁹

To summarize, the study of chiral molecules and surfaces is of great importance for finding safer alternatives to drugs. Here,

we have reported a different effect of two cysteine enantiomers on the attachment and growth of primary neurons. The L-Cys enantiomer seemed to be more toxic to the neurons than the D-Cys. Two settings were studied in our experiments: regenerating neurons in medium enriched with L-Cys and D-Cys, and regenerating neurons atop L-Cys and D-Cys SAM surfaces. In both settings, the L-Cys affected neuronal growth more significantly than the D-Cys that led to similar outgrowth pattern as the control. Exposure to the L-Cys enantiomer inhibited, and even prevented, neuronal attachment, in a concentration-dependent manner. Both approaches affected development of the neuronal branching tree, although the effect on the surfaces was delayed in comparison to treatment with cysteine solutions. Results from both settings demonstrate a different response of neurons to L-Cys vs D-Cys. The SAMs experimental assay demonstrates clearly that the sensitivity is to chirality. Neurons adhere better to the D-enantiomer, developing an elaborated dendritic tree. Interestingly, the addition of L-Cys as a free compound also affected neuronal adhesion. A possible explanation might be the L-Cys excitotoxicity that suggested as coupled to NMDA receptors²⁹ that have a role in neuronal membrane adhesion.⁵⁰

A protective role for D-Cys has been suggested, acting via different biochemical pathway than the L-Cys.⁵¹ Since the cysteine atop the SAMs is attached to the gold surface through a specific site, its thiol group, the neuronal membrane, interacts with the surface only via the Cys chiral sites. Previous studies have shown that the different effect of the two enantiomers can be related to different protein amounts absorbed on the surface which helps the cells adhere better to the L-enantiomer surface.^{15,48,52,53} It has been suggested that chiral molecules can affect proteins by noncovalent interaction^{54,55} such as stereoselective hydrophobic and hydrogen bonding effects.^{53,56} These effects may influence the interactions of cells with chiral

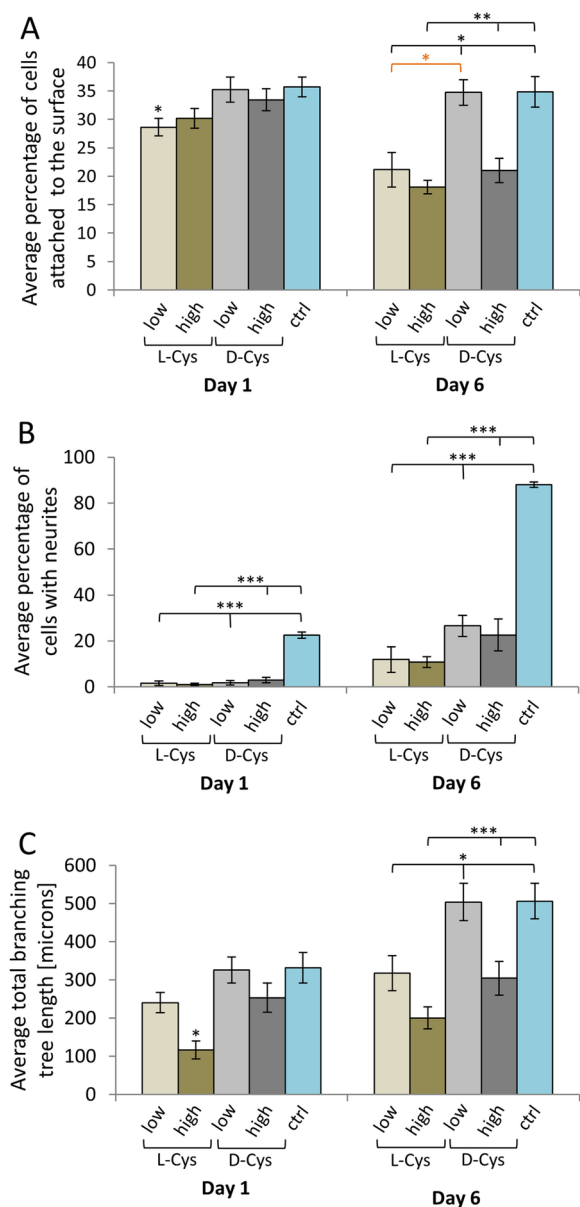


Figure 4. Statistics for neurons growing atop L- and D-Cys SAM surfaces. (A) Average percentage of cells attached to the SAM surfaces with low and high concentrations of L-Cys and D-Cys, and for the control, 1 day and 6 days after plating. (B) Average percentage of cells with neurites, for SAM surfaces with low and high concentrations of L-Cys and D-Cys, and for the control, 1 day and 6 days after plating. (C) Average total branching tree length for the SAM surfaces with low and high concentrations of L-Cys and D-Cys, and for the control, 1 day and 6 days after plating. Scheffe test, labeled in orange, comparison of two conditions $*p < 0.05$; GLM test, labeled in black, was used for multiple groups, $*p < 0.05$, $**p < 0.005$, $***p < 0.001$.

surfaces as we showed in our study, since neurons interact with the surface through the N-terminal hydrophobic group of the transmembrane receptors.

Our study demonstrates that the chiral site of the cysteine molecule may be the switch between the protective to the toxic interaction. The results suggest that chirality is important. L-Cys, which is required for normal brain function as an antioxidant compound and a neuromodulator, turns to be toxic at high levels, while D-Cys, with its concentration-dependent response manner, may provide a protective therapeutic route.

METHODS

Substrate Fabrication. Au films of 50 nm thickness (99.995%) were deposited on mica ($\text{KAl}_2(\text{AlSi}_3\text{O}_{10})(\text{OH})_2$) substrates using a high vacuum sputtering technique at a pressure of approximately 1×10^{-3} mbar with a deposition rate of 0.5 nm/s.

Figure 5 presents a typical atomic force microscopy (AFM) scan of the mica surface covered with a layer of ultraflat gold. The X-ray

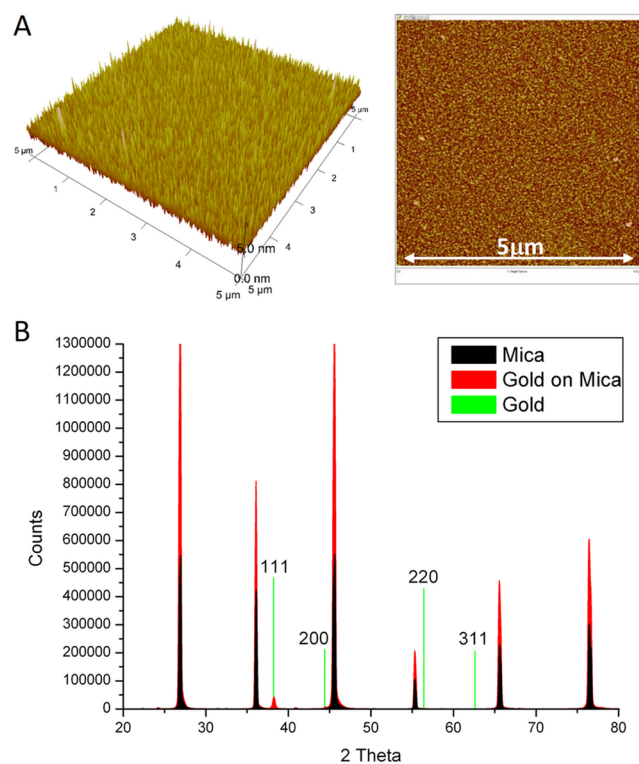


Figure 5. Substrate fabrication and characterization. (A) AFM images of the ultraflat gold covered mica surface. The topography of the gold–mica surfaces is very smooth (RMS: 0.48 nm). The gold films consist of small grains with typical sizes less than 60 nm. (B) X-ray diffraction (XRD) of Au-films. The X-ray diffraction of the gold surfaces shows a sharp peak at approximately $2\theta = 38^\circ$ corresponding to the (111) crystal plane orientation of gold. Other peaks (green lines) corresponding to orientations of gold other than (111) are not observed, indicating strong crystal orientation of the thin gold film. Additional peaks observed in the X-ray diffraction pattern correspond to the mica surface (black/red lines).

diffraction of the gold surfaces shows a sharp peak at approximately $2\theta = 38^\circ$ corresponding to the (111) crystal plane orientation of gold. Other peaks (green lines) corresponding to orientations of gold other than (111) were not observed, indicating strong crystal orientation of the thin gold film. The X-ray photoelectron spectroscopy of the chiral self-assembled monolayers shows peaks for nitrogen, sulfur and carbon, confirming the presence of cysteine on the surface (Supporting Information Figure S2). AFM measurements of the gold films show very smooth films with an average root-mean-square (RMS) roughness of 5 Å and with typical gold grain sizes of 60 nm (Figure 5A).

For the chiral SAMs, we used enantiomers of cysteine. Chiral SAMs were formed on gold surfaces by immersing the gold substrates overnight in 2 mM and 10 mM solutions of L- and D-Cys in deionized water. After removal from solutions, the chiral SAM surfaces were washed thoroughly with water and blown dry with nitrogen. Substrates were kept in dark until plating cells atop them. The formation and structure of the Cysteine SAMs on the gold surfaces were verified using various techniques: X-ray photoelectron spectroscopy (XPS), grazing angle Fourier transform infrared, and contact angle measure-

ments (see the Supporting Information). The stability of the SAM surfaces was previously detected, presenting high and long-term chemical stability for the duration of the experiments.³

Cell Culture. Culturing method has been previously described;⁴⁶ briefly, neurons were isolated from the CNS of adult medicinal leeches *Hirudo medicinalis*. Leeches were anaesthetized in 8% ethanol in leech Ringer before dissection. Nerve cords were dissected and ganglia were removed and pinned on Sylgard Petri dishes. Then, ganglia were treated enzymatically with 2 mg/mL collagenase/dispase enzyme solution (Roche, Mannheim, Germany) for 1 h at room temperature. Next, ganglia capsules were opened to expose the cells. Neuronal cells were rinsed and plated on the different substrates (see also schematic diagram in Figure 1). Neurons out of three ganglia (total of 1200 cells in a volume of 100 μ L) were plated on each substrate. For L- or D-Cys solution cultures, cysteine solutions were added to each culture accordingly (2 and 10 mM final concentrations in the medium). One day after plating, enriched medium was added to the cultures (Leibovitz L-15 supplemented with 6 mg/mL glucose, 0.1 mg/mL gentamycin, 2 mM/mL glutamine, and 2% fetal bovine serum), and L- and D-Cys was added to reach the right concentration (2 mM and 10 mM) in the culture medium. As for L-Cys, D-Cys and control substrates, only enriched medium was added to the cultures. Control substrates (not the L- and D-Cys substrates) were precoated with Concanavalin-A (Con-A) (Sigma-Aldrich Co., Saint Louis, MO, 0.5 mg/mL). Plates were kept in a 25 °C incubator for up to 2 weeks. Neuronal growth was followed during this period.

High Resolution Scanning Electron Microscopy. Six days after plating, neurons growing atop the L- and D-Cys substrates were fixed using 2.5% paraformaldehyde/2.5% glutaraldehyde in 0.1M sodium cacodylate buffer for 1 h at room temperature. After fixation, cultures were repeatedly rinsed in PBS (no Ca^{2+} , no Mg^{2+} , pH 7.2) and then treated with guanidine-HCl/tannic acid (4:5) solution (2%) for 1 h at room temperature. Cultures were repeatedly rinsed in PBS and then dehydrated in graded series of ethanol (50%, 70%, 80%, 90%, and 100%) and finally with graded series of Freon (50%, 75%, 100% \times 3). At the end, the preparations were dried and sputtered with carbon before examination by HR-SEM (Magellan 400L, FEI, Hillsboro, OR).

Morphometric Analysis. We measured the morphometric parameters of neurons on the different chiral substrates and compared them to neurons on the control substrates. Figure 1D demonstrates the morphometric parameters measured: the number of neurons attached to the substrate, the number of neurons with neurites and the neurite's total branching tree length. Attached neurons and neurons with neurites were measured manually. To measure process length we used NeuronJ,⁵⁷ an ImageJ plugin (US National Institutes of Health, Bethesda, MD), which enables semiautomatic tracing of neurites and length measurements.

Statistical Analysis. A minimum of three plates were considered for each substrate for the purpose of analysis. Neurons out of 3 ganglia per culture dish were plated (as described in the Cell Culture subsection). All neurons were measured for adhesion rate and outgrowth rate. The total branching tree lengths were measured for all neurons that developed neurites. Measurements of the morphometric parameters were summarized in bar charts. Error bars represent standard errors. In order to test the differences in frequency morphology for the various group types, the GLM procedure was performed, followed by Scheffe's test. *P*-values are presented for each parameter measured.

■ ASSOCIATED CONTENT

● Supporting Information

Electrophysiological recordings of neurons growing in culture medium supplemented with L-Cys and D-Cys solutions (Figure S1). Chiral SAM substrates characterization (Figures S2 and S3). This material is available free of charge via the Internet at <http://pubs.acs.org>.

■ AUTHOR INFORMATION

Corresponding Author

*E-mail: orit.shefi@biu.ac.il. Phone/Fax: +97235317079.

Funding

This work was partially supported by EU-FP7 People IRG Grant 239482 and the Israel Science Foundation Grant #1403/11 (O.S.) and by The Israeli Ministry of Science, Technology, and Space (K.B.).

Notes

The authors declare no competing financial interest.

■ ACKNOWLEDGMENTS

The authors wish to thank Yitzhak Mastai for his invaluable advice and fruitful discussions along the study.

■ ABBREVIATIONS

L-Cys, L-cysteine; D-Cys, D-cysteine; GSH, glutathione; CNS, central nervous system; SAMs, self-assembled monolayers; Con-A, concanavalin-A

■ REFERENCES

- (1) Pasteur, L. (1858) *C. R. Acad. Sci.* 46, 615.
- (2) Agranat, I., Caner, H., and Caldwell, J. (2002) Putting chirality to work: the strategy of chiral switches. *Nat. Rev. Drug Discovery* 1, 753–768.
- (3) Dressler, D. H., and Mastai, Y. (2007) Chiral crystallization of glutamic acid on self assembled films of cysteine. *Chirality* 19, 358–365.
- (4) Kitzerow, H. S., and Bahr, C. (2001) *Chirality in liquid crystals*, Springer, New York.
- (5) Mateos-Timoneda, M. A., Crego-Calama, M., and Reinhoudt, D. N. (2004) Supramolecular chirality of self-assembled systems in solution. *Chem. Soc. Rev.* 33, 363–372.
- (6) Dressler, D. H., and Mastai, Y. (2007) Enantioselective crystallization of histidine on chiral self-assembled films of cysteine. *J. Colloid Interface Sci.* 310, 653–660.
- (7) Mastai, Y. (2009) Enantioselective crystallization on nanochiral surfaces. *Chem. Soc. Rev.* 38, 772–780.
- (8) Rampulla, D., and Gellman, A. J. (2004) Enantioselectivity on Surfaces with Chiral Nanostructures. In *Dekker Encyclopedia of Nanoscience and Nanotechnology* (Schwarz, J. A., Contescu, C. I., and Putyera, K., Eds.), pp 1113–1123, Marcel Dekker, New York.
- (9) Hanein, D., Geiger, B., and Addadi, L. (1994) Differential adhesion of cells to enantiomorphous crystal surfaces. *Science* 263, 1413–1416.
- (10) Hanein, D., Yarden, A., Sabanay, H., Addadi, L., and Geiger, B. (1996) Cell-adhesion to crystal surfaces. Adhesion-induced physiological cell death. *Cell Adhes. Commun.* 4, 341–354.
- (11) Bandyopadhyay, D., Prashar, D., and Luk, Y. Y. (2011) Stereochemical effects of chiral monolayers on enhancing the resistance to mammalian cell adhesion. *Chem. Commun. (Cambridge, U.K.)* 47, 6165–6167.
- (12) El-Gindi, J., Benson, K., De Cola, L., Galla, H. J., and Kehr, N. S. (2012) Cell adhesion behavior on enantiomerically functionalized zeolite L monolayers. *Angew. Chem., Int. Ed. Engl.* 51, 3716–3720.
- (13) Sun, T., Han, D., Riehemann, K., Chi, L., and Fuchs, H. (2007) Stereospecific interaction between immune cells and chiral surfaces. *J. Am. Chem. Soc.* 129, 1496–1497.
- (14) Wang, X., Gan, H., Sun, T., Su, B., Fuchs, H., Vestweber, D., and Butz, S. (2010) Stereochemistry triggered differential cell behaviours on chiral polymer surfaces. *Soft Matter* 6, 3851–3855.
- (15) Zhang, M., Qing, G., and Sun, T. (2012) Chiral biointerface materials. *Chem. Soc. Rev.* 41, 1972–1984.
- (16) Shepard, P. D., Connelly, S. T., Lehmann, H., and Grobaski, K. C. (1995) Effects of the enantiomers of (\pm)-HA-966 on dopamine

neurons: an electrophysiological study of a chiral molecule. *Eur. J. Pharmacol.* 285, 79–88.

(17) Beutler, E. (1989) Nutritional and metabolic aspects of glutathione. *Annu. Rev. Nutr.* 9, 287–302.

(18) Kendall, E. C., Mason, H. L., and McKenzie, B. F. (1930) A study of glutathione. *J. Biol. Chem.* 88, 409–423.

(19) Kranich, O., Hamprecht, B., and Dringen, R. (1996) Different preferences in the utilization of amino acids for glutathione synthesis in cultured neurons and astroglial cells derived from rat brain. *Neurosci. Lett.* 219, 211–214.

(20) Brosnan, J. T., and Brosnan, M. E. (2006) The sulfur-containing amino acids: an overview. *J. Nutr.* 136, 1636S–1640S.

(21) Keller, H. J., Do, K. Q., Zollinger, M., Winterhalter, K. H., and Cuenod, M. (1989) Cysteine: depolarization-induced release from rat brain in vitro. *J. Neurochem.* 52, 1801–1806.

(22) Nelson, M. T., Joksovic, P. M., Perez-Reyes, E., and Todorovic, S. M. (2005) The endogenous redox agent L-cysteine induces T-type Ca²⁺ channel-dependent sensitization of a novel subpopulation of rat peripheral nociceptors. *J. Neurosci.* 25, 8766–8775.

(23) Sagara, J. I., Miura, K., and Bannai, S. (1993) Maintenance of neuronal glutathione by glial cells. *J. Neurochem.* 61, 1672–1676.

(24) Zangerle, L., Cuenod, M., Winterhalter, K. H., and Do, K. Q. (1992) Screening of thiol compounds: depolarization-induced release of glutathione and cysteine from rat brain slices. *J. Neurochem.* 59, 181–189.

(25) Dingledine, R., Borges, K., Bowie, D., and Traynelis, S. F. (1999) The glutamate receptor ion channels. *Pharmacol. Rev.* 51, 7–61.

(26) Pace, J. R., Martin, B. M., Paul, S. M., and Rogawski, M. A. (1992) High concentrations of neutral amino acids activate NMDA receptor currents in rat hippocampal neurons. *Neurosci. Lett.* 141, 97–100.

(27) Sullivan, J. M., Traynelis, S. F., Chen, H. S., Escobar, W., Heinemann, S. F., and Lipton, S. A. (1994) Identification of two cysteine residues that are required for redox modulation of the NMDA subtype of glutamate receptor. *Neuron* 13, 929–936.

(28) Gazit, V., Ben-Abraham, R., Coleman, R., Weizman, A., and Katz, Y. (2004) Cysteine-induced hypoglycemic brain damage: an alternative mechanism to excitotoxicity. *Amino Acids* 26, 163–168.

(29) Mathisen, G. A., Fonnum, F., and Paulsen, R. E. (1996) Contributing mechanisms for cysteine excitotoxicity in cultured cerebellar granule cells. *Neurochem. Res.* 21, 293–298.

(30) Puka-Sundvall, M., Eriksson, P., Nilsson, M., Sandberg, M., and Lehmann, A. (1995) Neurotoxicity of cysteine: interaction with glutamate. *Brain Res.* 705, 65–70.

(31) Saez, G., Thornalley, P. J., Hill, H. A., Hems, R., and Bannister, J. V. (1982) The production of free radicals during the autoxidation of cysteine and their effect on isolated rat hepatocytes. *Biochim. Biophys. Acta* 719, 24–31.

(32) Schoneich, C. (2008) Mechanisms of protein damage induced by cysteine thiyl radical formation. *Chem. Res. Toxicol.* 21, 1175–1179.

(33) Vina, J., Romero, F. J., Saez, G. T., and Pallardo, F. V. (1983) Effects of cysteine and N-acetyl cysteine on GSH content of brain of adult rats. *Experientia* 39, 164–165.

(34) Janáky, R., Varga, V., Hermann, A., Saransaari, P., and Oja, S. S. (2000) Mechanisms of L-cysteine neurotoxicity. *Neurochem. Res.* 25, 1397–1405.

(35) Slivka, A., and Cohen, G. (1993) Brain ischemia markedly elevates levels of the neurotoxic amino acid, cysteine. *Brain Res.* 608, 33–37.

(36) Todorovic, S. M., Jevtovic-Todorovic, V., Meyenburg, A., Mennerick, S., Perez-Reyes, E., Romano, C., Olney, J. W., and Zorumski, C. F. (2001) Redox modulation of T-type calcium channels in rat peripheral nociceptors. *Neuron* 31, 75–85.

(37) Todorovic, S. M., Meyenburg, A., and Jevtovic-Todorovic, V. (2004) Redox modulation of peripheral T-type Ca²⁺ channels in vivo: alteration of nerve injury-induced thermal hyperalgesia. *Pain* 109, 328–339.

(38) Ferkany, J., and Coyle, J. T. (1986) Heterogeneity of sodium-dependent excitatory amino acid uptake mechanisms in rat brain. *J. Neurosci. Res.* 16, 491–503.

(39) Skandali, N. (2009) L-Cysteine against heavy metal neurotoxicity. *Adv. Altern. Thinking Neurosci.* 1, 15–20.

(40) Wang, X. F., and Cynader, M. S. (2000) Astrocytes provide cysteine to neurons by releasing glutathione. *J. Neurochem* 74, 1434–1442.

(41) Wang, X. F., and Cynader, M. S. (2001) Pyruvate released by astrocytes protects neurons from copper-catalyzed cysteine neurotoxicity. *J. Neurosci.* 21, 3322–3331.

(42) Emes, R. D., Wang, W. Z., Lanary, K., and Blackshaw, S. E. (2003) HmCRIP, a cysteine-rich intestinal protein, is expressed by an identified regenerating nerve cell. *FEBS Lett.* 533, 124–128.

(43) Fuchs, S. A., Berger, R., Klomp, L. W., and de Koning, T. J. (2005) D-amino acids in the central nervous system in health and disease. *Mol. Genet. Metab.* 85, 168–180.

(44) Yamane, H., Asechi, M., Tsuneyoshi, Y., Denbow, D. M., and Furuse, M. (2009) Central L-cysteine induces sleep, and D-cysteine induces sleep and abnormal behavior during acute stress in neonatal chicks. *Anim. Sci. J.* 80, 428–432.

(45) Patil, P. A., and Kothekar, M. A. (2006) Development of safer molecules through chirality. *Indian J. Med. Sci.* 60, 427–437.

(46) Baranes, K., Chejanovsky, N., Alon, N., Sharoni, A., and Shefi, O. (2012) Topographic cues of nano-scale height direct neuronal growth pattern. *Biotechnol. Bioeng.* 109, 1791–1797.

(47) Gillin, F. D., and Diamond, L. S. (1980) Attachment of *Entamoeba histolytica* to glass in a defined maintenance medium: specific requirement for cysteine and ascorbic acid. *J. Protozool.* 27, 474–478.

(48) Zhou, F., Yuan, L., Li, D., Huang, H., Sun, T., and Chen, H. (2012) Cell adhesion on chiral surface: the role of protein adsorption. *Colloids Surf., B* 90, 97–101.

(49) Yao, X., Hu, Y., Cao, B., Peng, R., and Ding, J. (2013) Effects of surface molecular chirality on adhesion and differentiation of stem cells. *Biomaterials* 34, 9001–9009.

(50) Husi, H., Ward, M. A., Choudhary, J. S., Blackstock, W. P., and Grant, S. G. (2000) Proteomic analysis of NMDA receptor-adhesion protein signaling complexes. *Nat. Neurosci.* 3, 661–669.

(51) Shibuya, N., and Kimura, H. (2013) Production of hydrogen sulfide from D-cysteine and its therapeutic potential. *Front. Endocrinol.* 4, 87.

(52) Chen, Q., Zhou, J., Han, Q., Wang, Y., and Fu, Y. (2012) The selective adsorption of human serum albumin on N-isobutyl-L-cysteine enantiomers modified chiral surfaces. *Biochem. Eng. J.* 69, 155–158.

(53) Wang, X., Gan, H., and Sun, T. (2011) Chiral design for polymeric biointerface: the influence of surface chirality on protein adsorption. *Adv. Funct. Mater.* 21, 3276–3281.

(54) Inai, Y., Ousaka, N., and Ookouchi, Y. (2006) Chiral interaction in peptide molecules: effects of chiral peptide species on helix-sense induction in an N-terminal-free achiral peptide. *Biopolymers* 82, 471–481.

(55) Inai, Y., Komori, H., and Ousaka, N. (2007) Control of helix sense in protein-mimicking backbone by the noncovalent chiral effect. *Chem. Rec.* 7, 191–202.

(56) Tang, K., Gan, H., Li, Y., Chi, L., Sun, T., and Fuchs, H. (2008) Stereoselective interaction between DNA and chiral surfaces. *J. Am. Chem. Soc.* 130, 11284–11285.

(57) Meijering, E., Jacob, M., Sarria, J. C., Steiner, P., Hirling, H., and Unser, M. (2004) Design and validation of a tool for neurite tracing and analysis in fluorescence microscopy images. *Cytometry, Part A* 58, 167–176.